

The Effect of Alcohol Consumption on Brain Ageing: A New Causal Inference Framework for Incomplete and Massive Phenomic Data

Chixiang Chen^{1*}, Shuo Chen¹, Zhenyao Ye¹, Xu Shi², Tianzhou Ma³

¹ Division of Biostatistics and Bioinformatics,

University of Maryland School of Medicine, Baltimore, U.S.A.

²Department of Biostatistics, University of Michigan, Ann Arbor, U.S.A.

³Department of Epidemiology and Biostatistics,

University of Maryland, College Park, U.S.A.

March 5, 2024

Abstract

Although substance use, such as alcohol consumption, is known to be associated with cognitive decline during ageing, its direct influence on the central nervous system remains unclear. In this study, we aim to investigate the potential influence of alcohol intake frequency on accelerated brain ageing by estimating the mean potential brain—age gap (BAG) index, the difference between brain age and actual age, under different alcohol intake frequencies in a large UK Biobank (UKB) cohort with extensive phenomic data reflecting a comprehensive life-style profile. We face two major challenges: (1) a large number of phenomic variables as potential confounders and (2) a small proportion of participants with complete phenomic data. To address these challenges, we first develop a new ensemble learning framework to establish robust estimation of mean potential outcome in the presence of many confounders. We then construct a data integration step to borrow information from UKB participants with incomplete phenomic data to improve efficiency. Our analysis results reveal that daily intake or even a few times a week may have significant effects on accelerating brain ageing. Moreover, extensive numerical studies demonstrate the superiority of our method over competing methods, in terms of smaller estimation bias and variability.

Keywords: Brain ageing; Data integration; Ensemble learning; Phenomics; Robustness.

*Contact: chixiang.chen@som.umaryland.edu

1 Introduction

The availability of high-dimensional phenotypic data, referred to as phenomic data, offers new opportunities to study physical and biochemical traits of the organism (Houle et al. 2010). Our study is highly motivated by the investigation of the potential influence of substance use, such as alcohol intake, on white matter brain ageing, as characterized by neuroimaging techniques. Although recent literature have been shown that high level of alcohol intake will increase the risk of accelerated cognitive decline and all-cause mortality during ageing (Mende 2019, Zhao et al. 2023), the direct influence of alcohol consumption on the central nervous system remains unclear. In the recent literature of neuroimaging research, the concept of ‘brain age’ has garnered increased interest, which calculates the neurobiological condition of ageing brain based on neuroimaging data. Due to numerous genetic and environmental factors, imaging-based brain age may differ from the chronological age. The difference between brain age and actual age, called the brain–age gap (BAG), provides a new measure of whether a subject’s brain appears to have aged more or less than his chronological age (Smith et al. 2019, Mo et al. 2022). Our goal is to estimate the mean of potential BAG index value under different alcohol intake frequencies, with the value larger than zero indicating brain ageing. To unbiasedly identify the impact of varying alcohol intake frequencies on brain ageing, it is essential to account for phenomic variables such as demographics, social status, lifestyle, and health conditions (Mende 2019).

To account for a sufficient number of factors that confound the relationship between alcohol intake and the BAG index, we use data from the UK Biobank, which provides phenomic data with unprecedented breadth and depth, including subtle measurements that are absent in most studies such as multimodal brain imaging, nutrition intake and physical activities, and comprehensive blood measures and metabolomics. These phenomic variables

jointly reflect a comprehensive life-style profile. After data processing, however, barely above 2800 participants have the full set of phenomic data observed in the study of alcohol consumption (as the main data), while much more participants miss massive phenomic data in both studies (around 19000 participants as the auxiliary data). To simultaneously achieve an unbiased and efficient estimation, we face two statistical challenges: (1) how to handle massive phenomic variables in the main data with unknown and complex confounding effects? (2) how to boost efficiency of estimating the mean potential outcome in the main data, possibly by borrowing information from the auxiliary data with a large sample size?

The literature describes many techniques to handle observed confounders, including conditional mean imputation (Robins 1999), (augmented) inverse probability weighting (Horvitz & Thompson 1952, Robins et al. 1994, Bang & Robins 2005, Han & Wang 2013), and matching (Rubin 1973, 2006, Antonelli et al. 2018). Most methods require specification and estimation of nuisance functions, such as the conditional mean and/or propensity score model. When handling many covariates and complex non-linear confounding effects in estimating these nuisance functions, causal machine learning methods using random forest or gradient boosting are preferred to classic regression and lead to tractable statistical properties (Chernozhukov et al. 2018, Yang et al. 2023, Cui et al. 2023). Despite substantial efforts, a considerable concern when using existing machine-learning-based methods relates to having prior knowledge of the best one to use, in the presence of multiple machine learning algorithms. Machine learning algorithms have a black-box characteristic, and their performance can substantially vary across databases and underlying set-ups. Although advanced computational schemes such as super-learning and ENSEMBLE (Polley & Van der Laan 2010, Ganaie et al. 2021) are numerically capable of integrating multiple machine learning algorithms, these methods require sophisticated coding skills and much

larger databases for training, validation, and testing, which may not be suitable in our applications (e.g., 2800 participants in the study of alcohol consumption). Therefore, how to effectively integrate multiple machine learning models and robustly estimate the population mean potential outcome is still open to research.

On the other hand, a promising attempt to overcome the issue of small sample size is to integrate information from external data or auxiliary records within the data. In the past decades, researchers have employed many different information integration schemes, such as meta-analysis, generalized-meta analysis, empirical likelihood method, constrained maximum likelihood method, and Bayesian method with informative prior (Qin & Lawless 1994, Qin et al. 2015, Chatterjee et al. 2016, Kundu et al. 2019, Cheng et al. 2019, Yang & Ding 2019, Zhang et al. 2020, Jiang, Nie & Yuan 2021, Zhai & Han 2022, Sheng et al. 2022, Chen et al. 2022). Most of the methods mentioned above use summary information extracted from external sources and have not been applied to the context of causal inference. In our applications, a few participants form the main data, while numerous participants who miss massive phenomic variables form the auxiliary data. Integrating information from this auxiliary data to boost efficiency of estimating mean potential outcome in the main data is substantially interesting and not well explored in literature.

To simultaneously and robustly handle the issues of complex confounding and small sample size, we propose a new statistical framework with an ensemble learner that is robust and efficient (Figure 1A). This learner has several unique advantages over aforementioned methods. First, our learner allows multiple machine learning algorithms to model the nuisance functions, in contrast to the work in Han & Wang (2013) using generalized linear model with applications in missing data. The resulting estimator is robust in the sense that it is consistent if one algorithm captures the true propensity score and one algorithm

captures the true conditional mean. This learner leads to oracle convergence rate and tractable statistical properties (Chernozhukov et al. 2018) and does not require extra independent data to fulfill model ensemble or prior knowledge about the best algorithm, which is particularly useful when the main data is not very large. Second, the proposed learner leads to high estimation efficiency by integrating information from auxiliary data. In our application, the auxiliary data include study participants whose phenomic data are only partially observed. This case can also be viewed as an extreme missing data problem due to massive unobserved covariates, and traditional missing-data techniques such as imputation may not fit well. Herein, we develop a novel data integration scheme that efficiently uses such auxiliary data to boost the estimation efficiency of the learner, by proposing novel informative scores via empirical likelihood (Qin & Lawless 1994). This new integration scheme is computationally convenient and can flexibly handle a multi-categorical exposure. Furthermore, the application of this new statistical framework leads to interesting scientific findings in studies of alcohol intake frequency on brain ageing.

The remaining sections of this paper are organized as follows. Section 2 describes used notations in the manuscript. Section 3 illustrates the new framework of robust machine learner and data integration along with theoretical properties. Section 4 presents a case study about the impact of alcohol consumption on mean potential outcome estimation of BAG. Section 5 includes extensive numerical evaluations of the proposed estimator. Section 6 discusses extensions of our method. All technical proofs, numerical procedures, and extra real data results and simulations can be found in the Supplementary Material.

2 Notation

For $i = 1, \dots, n$, let $(Y_i, X_i, \mathbf{Z}_i^\top)^\top$ be the independent and identically distributed data for subject i , where Y is a univariate outcome of interest, $X = x \in \{0, \dots, L\}$ is a univariate exposure variable with in total $L + 1 \geq 2$ levels, and \mathbf{Z} is a p -dimensional vector consisting of observed confounders of the outcome Y and exposure X . In addition to the main data, we consider an auxiliary dataset: for $i = n + 1, \dots, N$, let $(Y_i, X_i)^\top$ be the independent and identically distributed auxiliary data. We focus on the scenario where the raw auxiliary data Y and X are available, whereas the variables in \mathbf{Z} are not observed at all or only partially observed. These variables follow the same joint distribution of the main data, i.e., the main and auxiliary data are from the same population. This assumption has been widely adopted in studies reported in the literature (Zhang et al. 2020, Jiang, Yang, Qin & Zhou 2021). The violation of this homogeneous assumption will be discussed in Sections 3.3, 5, and 6. Moreover, under the Stable Unit Treatment Value Assumption, let $Y_i(x)$ be the potential outcome of the subject i if the exposure status had, possibly contrary to fact, been set to $X = x$. Then the population mean potential outcome is defined as

$$\tau(x) = E\{Y(x)\}. \quad (1)$$

We further use $\mu_x = E(Y|X = x, \mathbf{Z})$ and $\pi_x = Prob(X = x|\mathbf{Z})$ to denote the conditional mean (CM) of the outcome given exposure status $X = x$ and confounders \mathbf{Z} and the conditional probability of $X = x$ given confounders \mathbf{Z} , respectively. In the literature, π_x is often referred to as the (generalized) propensity score (PS) (Rosenbaum & Rubin 1983). The fundamental problem in causal inference is that we only observe at most one potential outcome for a subject. Thus, to identify $\tau(x)$, we require the following two assumptions.

Assumption 1 (no unmeasured confounding): $Y(x) \perp\!\!\!\perp X|\mathbf{Z}$, for $x = 0, \dots, L$.

Assumption 2 (positivity): $0 < \pi_x < 1$, for $x = 0, \dots, L$.

Under Assumption 1, we require that the exposure assignment can be ignored, i.e., there is no unmeasured confounding; under Assumption 2, we require adequate overlap of covariate distributions among $x = 0, \dots, L$. These two assumptions are widely adopted in causal-inference studies (Rosenbaum & Rubin 1983, Yang & Ding 2019). In the remainder of this article, we propose a unified framework with causal machine learning and data integration to estimate population mean potential outcomes in exposure groups, showing robust estimation with reduced variability.

3 Method

3.1 Augmented inverse probability treatment weighting

We first briefly review a well-known estimator, the augmented inverse probability treatment weighting (AIPTW). The AIPTW estimator is as follows:

$$\hat{\tau}_{\text{aiptw}}(x) = \frac{1}{n} \sum_{i=1}^n \left\{ \frac{I(X_i = x)}{\hat{\pi}_{xi}} Y_i - \frac{I(X_i = x) - \hat{\pi}_{xi}}{\hat{\pi}_{xi}} \hat{\mu}_{xi} \right\} \text{ for } x = 0, \dots, L, \quad (2)$$

where $I(E)$ is an indicating function that takes a value of 1 if event E happens and 0 otherwise. Specifically, the term $\{I(X_i = x)/\hat{\pi}_{xi}\}Y_i$ corresponds to the estimated inverse probability treatment weighting method accounting for imbalanced distribution of exposure assignment. On the other hand, the term $[\{I(X_i = x) - \hat{\pi}_{xi}\}/\hat{\pi}_{xi}]\hat{\mu}_{xi}$ is the so-called augmentation term that incorporates auxiliary information from covariates \mathbf{Z}_i through the estimated conditional mean $\hat{\mu}_{xi}$. A conventional approach to estimate the PS model and CM model is to specify parametric models $\pi_x(\boldsymbol{\alpha})$ and $\mu_x(\boldsymbol{\xi})$ with parameters $\boldsymbol{\alpha}$ and $\boldsymbol{\xi}$ solved by regression methods such as the generalized linear model (Nelder & Wedderburn 1972). Moreover, it has been shown that $\hat{\tau}_{\text{aiptw}}$ is doubly robust, i.e., it is consistent if either the PS model or the CM model holds, not necessarily both (Bang & Robins 2005). When

both models are correctly specified, $\hat{\tau}_{\text{aiptw}}$ is semiparametric efficient (Robins et al. 1994). However, when both models are wrong, $\hat{\tau}_{\text{aiptw}}$ can lead to substantial bias, i.e., two wrong models are not better than one (Kang & Schafer 2007). The latter situation is not unlikely when using generalized linear models to fit, as parametric models are too stringent when analyzing a large-scale and complex observational database.

To alleviate the curse of dimensionality but still achieve tractable statistical properties, it may be beneficial to leverage machine learning algorithms into the AIPTW framework, such as penalized regression and random forest, that can fit richly parameterized models with flexible functional forms for the variables in \mathbf{Z}_i (Hernán & Robins 2010, Chernozhukov et al. 2018). However, given the numbers of computational techniques available on the market, it is difficult to identify the best algorithm that leads to the most reliable result in practice. This motivates the ensemble of multiple machine learning algorithms which we detail in the next subsection. We note here that the most complicated model does not necessarily lead to the best estimate. When the true model is known and has linear structure, conventional regression will have the desired statistical property and may perform better numerically than a complicated model based on machine learning algorithms. We refer readers to Section 5 for more numerical evidence (Table 2).

3.2 Robust weighting with machine learning

In this section, we propose a learner that allows multiple machine learning algorithms to fit the PS and CM models and leads to valid statistical inference. This learner implicitly implements model ensemble or prior knowledge of the best algorithm, without requiring extra data to fulfill model ensemble.

Before presenting the proposed learning procedure, we first introduce more notation.

For $x = 0, \dots, L$, let $\hat{\pi}_{xi}^{(1)}, \dots, \hat{\pi}_{xi}^{(J_1)}$ be the estimates of PS for subject i based on a total of J_1 candidate algorithms. For example, $\hat{\pi}_{xi}^{(1)}$ is learned by logistic regression, $\hat{\pi}_{xi}^{(2)}$ is learned by regression with l_2 -penalty, $\hat{\pi}_{xi}^{(3)}$ is learned by random forest, and $\hat{\pi}_{xi}^{(4)}$ is learned by gradient boosting. Similarly, let $\hat{\mu}_{xi}^{(1)}, \dots, \hat{\mu}_{xi}^{(J_2)}$ be the estimates of CM based on J_2 candidate algorithms. Given all candidates, our robust causal machine learning (CML) estimator is built upon the following weighted estimation:

$$\hat{\tau}_{\text{cml}}(x) = \sum_{i \in \{i|X_i=x\}} \hat{\omega}_{xi} Y_i, \text{ for } x = 0, \dots, L, \quad (3)$$

where the estimated weight $\hat{\omega}_{xi}$ is solved by maximizing $\prod_{i \in \{i|X_i=x\}} \omega_{xi}$ with respect to constraints $\omega_{xi} > 0$, $\sum_{i \in \{i|X_i=x\}} \omega_{xi} = 1$, and $\sum_{i \in \{i|X_i=x\}} \omega_{xi} \hat{\mathbf{g}}_{xi} = \mathbf{0}$, with

$$\hat{\mathbf{g}}_{xi} = \left(\hat{\pi}_{xi}^{(1)} - \frac{1}{n} \sum_{l=1}^n \hat{\pi}_{xl}^{(1)}, \dots, \hat{\pi}_{xi}^{(J_1)} - \frac{1}{n} \sum_{l=1}^n \hat{\pi}_{xl}^{(J_1)}, \right. \\ \left. \hat{\mu}_{xi}^{(1)} - \frac{1}{n} \sum_{l=1}^n \hat{\mu}_{xl}^{(1)}, \dots, \hat{\mu}_{xi}^{(J_2)} - \frac{1}{n} \sum_{l=1}^n \hat{\mu}_{xl}^{(J_2)} \right)^\top. \quad (4)$$

In particular, the constraint $\sum_{i \in \{i|X_i=x\}} \omega_{xi} \hat{\mathbf{g}}_{xi} = \mathbf{0}$ is imposed such that the weight $\hat{\omega}_{xi}$ calibrates the covariate distribution of the corresponding group to that of the entire population, thus leading to a consistent estimator of the population mean potential outcome $\tau(x)$. The original estimator was first proposed by Han & Wang (2013) under the context of missing data, in which generalized linear models was used to fit missing data and outcome conditional mean models. They proved that the resulting estimator was consistent if one of the $J_1 + J_2$ models was correctly specified and was less sensitive to extreme PS values compared to traditional PS weighting methods. In this paper, we broaden its use to causal inference with a multi-categorical exposure and by applying advanced machine learning.

However, the estimator from Han & Wang (2013) has oracle converge rate $O_p(n^{-1/2})$ only when the conventional statistical regression is considered to fit PS and CM. In the context of machine learning, this estimator may have a lower convergence rate, $O_p(n^{-\phi})$,

with $\phi < 1/2$ (Hernán & Robins 2010, Chernozhukov et al. 2018). The key driving force behind this behaviour is the bias in learning the true π_{xi} and μ_{xi} . Similar to non-parametric estimation, machine learning estimate prevents the variance of the estimator from exploding at the price of induced bias. As such, we have $\hat{\pi}_{xi}^{(j_1)} - \pi_{xi} = O_p(n^{-\phi_1})$, $j_1 = 1, \dots, J_1$ and $\hat{\mu}_{xi}^{(j_1)} - \mu_{xi} = O_p(n^{-\phi_2})$, $j_2 = 1, \dots, J_2$, with $\phi_1, \phi_2 < 1/2$. Therefore, $\hat{\tau}_{\text{cml}}(x)$ may have a slower convergence rate and thus be less desirable for use in various applications.

To achieve oracle convergence rate $O_p(n^{-1/2})$, a tractable asymptotic distribution for $\hat{\tau}_{\text{cml}}(x)$, and avoid potential over-fitting for PS and CM, we adopt the technique of sample splitting and cross-fitting and impose several assumptions described in Section 3.4. Specifically, we randomly split the data into a training set and an evaluation set, each with $n/2$ samples. We first apply predictive algorithms to samples in the training set to obtain the estimates $\hat{\pi}_{xi}^{(j_1)}$ and $\hat{\mu}_{xi}^{(j_2)}$ for $j_1 = 1, \dots, J_1$ and $j_2 = 1, \dots, J_2$, which are then evaluated on samples in the evaluation set to estimate $\hat{\tau}_{\text{cml}}(x)$. To fully make use of the data, we repeat the above procedure but swap the roles of the training and evaluation halves of the study sample; the final estimate will be the average of the two estimates for $\tau(x)$ from each half of the population. The above process avoids the use of the same set of outcomes in both PS & CM and mean potential outcome estimation, enabling valid statistical inference (Hernán & Robins 2010, Chatterjee et al. 2016).

3.3 Information integration

The proposed estimator, $\hat{\tau}_{\text{cml}}(x)$, in (3) is robust and has little bias under mild conditions (Section 3.4); thus, it successfully achieves our first goal, i.e., robustness. We now improve efficiency by integration information from auxiliary data on participants $i = n + 1, \dots, N$, while retaining robustness. We assume that p -dimensional vector \mathbf{Z} is not observed at

all or only partially observed in the auxiliary data. Thus, naively merging the main and auxiliary data and using observed variables is improper as it results in biased estimates for PS and CM. Given the complex nature of the CML estimator, integrating information from the auxiliary data requires a new estimation framework. To this end, we propose the following causal machine learning estimator with information borrowing (CMLIB)

$$\hat{\tau}_{\text{cmlib}}(x) = \sum_{i \in \{i|X_i=x\}} \frac{\hat{p}_i \hat{\omega}_{xi}^* Y_i}{\sum_{i \in \{i|X_i=x\}} \hat{p}_i \hat{\omega}_{xi}^*}. \quad (5)$$

In contrast to the estimator in (3), CMLIB incorporates two weights. One is \hat{p}_i (named “integration scores”), and the other is the calibration weights $\hat{\omega}_{xi}^*$. The insight of proposing (5) and the estimation procedure are summarized below:

Integration scores. Integration score is a new concept developed in this paper to deliver information from auxiliary data. Using both main and auxiliary data, the informative scores \hat{p}_i are estimated by maximizing $\prod_{i=1}^N p_i$ with respect to $p_i > 0$, $\sum_{i=1}^N p_i = N$, and $\sum_{i=1}^N p_i \mathbf{H}_i(\boldsymbol{\theta}) = \mathbf{0}$ with

$$\mathbf{H}_i(\boldsymbol{\theta}) = \begin{Bmatrix} R_i \mathbf{h}_i(\boldsymbol{\theta}) \\ (1 - R_i) \mathbf{h}_i(\boldsymbol{\theta}) \end{Bmatrix}. \quad (6)$$

Here, R_i is a data indicator that takes the value of 1 if $i = 1, \dots, n$ and 0 if $i = n+1, \dots, N$. The function $\mathbf{h}_i(\boldsymbol{\theta})$ is a “working” estimating function with a nuisance parameter vector $\boldsymbol{\theta}$ for both main and auxiliary data. Two remarks are highlighted: (1) the working function $\mathbf{h}_i(\boldsymbol{\theta})$ should be constructed only based on the observed variables from both data, and (2) different function forms may affect the integration performance. Herein, we introduce two simple forms (but not limited to these two in practice) that work well in our simulation and real data applications.

$$(I) h_i(\theta) = Y_i - \theta \text{ and } (II) \mathbf{h}_i(\boldsymbol{\theta}) = (1, X_i)^\top \{Y_i - (1, X_i)\boldsymbol{\theta}\}. \quad (7)$$

The latter function is based upon the notation with a binary exposure. The function in

the setting with a multi-categorical exposure can be similarly followed.

The intuition of proposing integration scores relies on the construction of over-identified estimating function in (6). Here, over-identification means that the length of indexed parameter vector $\boldsymbol{\theta}$ should be shorter than the length of the estimating function $\mathbf{H}_i(\boldsymbol{\theta})$. Motivated by empirical likelihood theory (Qin & Lawless 1994, Chen et al. 2022, 2023), an over-identified function will enable the resulting estimates \hat{p}_i encapsulating information from the used variables from both datasets, which implies a more efficient estimate of the distribution function of these variables than the simple empirical distribution function (Qin & Lawless 1994). As a result, these estimated scores \hat{p}_i serving as informative weights in (5) (compared to weights equal to 1) is expected to facilitate the transfer of information to the estimation of mean potential outcome.

We also remark here that the shared function $\mathbf{h}_i(\cdot)$ in both data implies that the main and auxiliary data are from the same population. The violation will lead to biased estimation for population mean potential outcome. In real cases where baseline and observed covariate distributions are not same in the main and auxiliary data, pre-screening the auxiliary data is recommended owing to inclusion and exclusion criteria in the main study. Also, PS matching can be implemented based on observed baseline covariates to correct imbalanced distributions between two datasets. More discussions of handling heterogeneous populations can be found in Section 5.3 and 6.

Calibration weights. These weights aim to balance covariate distributions in a robust manner. One naive attempt is to directly use the weights $\hat{\omega}_{xi}$ in (3). If so, however, variance reduction for the estimate in (5) cannot be ensured in asymptotic theory. To achieve efficiency gain, we consider the following modification: after obtaining integration scores \hat{p}_i , we can calculate the calibration weights $\hat{\omega}_{xi}^*$ by maximizing $\prod_{i \in \{i | X_i = x\}} \omega_{xi}^*$ with

respect to $\omega_{xi}^* > 0$, $\sum_{i \in \{i|X_i=x\}} \omega_{xi}^* = 1$, and $\sum_{i \in \{i|X_i=x\}} \omega_{xi}^* \hat{\mathbf{g}}_{xi}^* = \mathbf{0}$ with

$$\hat{\mathbf{g}}_{xi}^* = \left(\hat{\pi}_{xi}^{(1)} - \frac{1}{n} \sum_{l=1}^n \hat{\pi}_{xl}^{(1)}, \dots, \hat{\pi}_{xi}^{(J_1)} - \frac{1}{n} \sum_{l=1}^n \hat{\pi}_{xl}^{(J_1)}, \hat{p}_i \hat{\mu}_{xi}^{(1)} - \frac{1}{n} \sum_{l=1}^n \hat{p}_l \hat{\mu}_{xl}^{(1)} + (1 - \hat{p}_i) \hat{\eta}_x^{(1)}, \right. \\ \left. \dots, \hat{p}_i \hat{\mu}_{xi}^{(J_2)} - \frac{1}{n} \sum_{l=1}^n \hat{p}_l \hat{\mu}_{xl}^{(J_2)} + (1 - \hat{p}_i) \hat{\eta}_x^{(J_2)} \right)^\top \quad (8)$$

and $\hat{\eta}_x^{(j_2)} = (1/n) \sum_{l=1}^n \hat{\mu}_{xl}^{(j_2)}$, for $j_2 = 1, \dots, J_2$. The updated calibration function $\hat{\mathbf{g}}_{xi}^*$ in (8) incorporates integration scores \hat{p}_i and $(1 - \hat{p}_i) \hat{\eta}_x^{(j_2)}$, contrasting with the calibration function $\hat{\mathbf{g}}_{xi}$ in (4). This modification is rooted in mathematical reasoning aimed at ensuring reduced estimation variability. We refer readers to technical details in Section 1.2 of the Supplementary Material.

We remark here that the doubly weighted estimator in (5) serves as a generalization of the CML estimator in (3). Specifically, in scenarios without auxiliary data (i.e., when $N = n$), the integration scores will be reduced to 1 as per empirical likelihood theory (Qin & Lawless 1994). Consequently, the calibration weights $\hat{\omega}_{xi}^*$ in (5) will be reduced to $\hat{\omega}_{xi}$ in (3), i.e., no efficiency gain at all.

It is noteworthy that sample splitting and cross-fitting are unnecessary for calculating integration scores, but they are required for computing calibration weights. The complete learning procedure is summarized in Algorithm 1. As discussed in Section 3.4, the doubly weighted estimation in (5) asymptotically ensures enhanced efficiency in estimating the mean potential outcome, while preserving the robustness property.

3.4 Theoretical property

We first derive the asymptotic property of the estimator $\hat{\tau}_{\text{cml}}(x)$ in (3). In addition to regular and well-recognized conditions from the empirical likelihood literature (Qin & Lawless 1994), we need the following assumptions to facilitate our derivation. Given any values of

Algorithm 1: Estimation Procedure

Data: Main data $(Y_i, X_i, \mathbf{Z}_i)_{i=1}^n$ and Auxiliary data $(Y_i, X_i)_{i=n+1}^N$;

if Auxiliary data are not available **then**

Set $\hat{p}_i \leftarrow 1$, for $i = 1, \dots, n$;

else

Informative scores: Obtain the scores \hat{p}_i by (6) of the manuscript based on both main data and auxiliary data ;

Processed Data: Randomly split the data into two halves, denoted by data 1 and data 2;

for each data $i \in \{1, 2\}$ **do**

Apply different candidate algorithms to learn $\hat{\pi}_x$ and $\hat{\mu}_x$ based on data i ;

Calculate the estimator $\hat{\tau}_{\text{cmlib}}(x; j)$ based on (5) and the data j , $j \neq i$;

end

end

Result: Obtain the final estimator $\hat{\tau}_{\text{cmlib}}(x) = \{\hat{\tau}_{\text{cmlib}}(x; 1) + \hat{\tau}_{\text{cmlib}}(x; 2)\}/2$.

\mathbf{Z} , let $\pi_{xi}^{(j_1)}$ denote the limiting value of $\hat{\pi}_{xi}^{(j_1)}$, and let $\mu_{xi}^{(j_2)}$ denote the limiting value of $\hat{\mu}_{xi}^{(j_2)}$, for $j_1 = 1, \dots, J_1$ and $j_2 = 1, \dots, J_2$.

Assumption 3 (well-behaved estimates). $n^{-0.5} \sum_{i=1}^n \boldsymbol{\epsilon}_{xi} \boldsymbol{\epsilon}_{xi}^\top = o_p(\mathbf{1})$, where $\boldsymbol{\epsilon}_{xi} = (\hat{\pi}_{xi}^{(1)} - \pi_{xi}^{(1)}, \dots, \hat{\pi}_{xi}^{(J_1)} - \pi_{xi}^{(J_1)}, \hat{\mu}_{xi}^{(1)} - \mu_{xi}^{(1)}, \dots, \hat{\mu}_{xi}^{(J_2)} - \mu_{xi}^{(J_2)})^\top$.

Assumption 4 (robust learning). There exist $j_1 \in \{1, \dots, J_1\}$ and $j_2 \in \{1, \dots, J_2\}$ such that $\pi_{xi}^{(j_1)} = \pi_{xi}$ and $\mu_{xi}^{(j_2)} = \mu_{xi}$, where π_{xi} and μ_{xi} are the true PS and CM, respectively.

The first assumption requires well-behaved estimates from all candidate algorithms. As we do not require these limiting values to be the true PS and CM, this assumption is much milder than requiring all estimates to converge to the true value. Moreover, the individual convergence rates of PS and CM estimates can be slower than $O_p(n^{-0.5})$, as long as their residual products exhibit convergence rates faster than $O_p(n^{-0.5})$. Consequently, Assumption 3 encompasses a broader class of PS and CM estimates and is an extension of

commonly used assumption in the context of causal machine learning (Chernozhukov et al. 2018, Jiang et al. 2022, Yang et al. 2023).

Assumption 4, on the other hand, does not require an oracle guess or *a priori* knowledge about the best algorithm; instead, it only requires the existence of two candidate algorithms among others that can capture the true PS and CM, respectively. We summarize the asymptotic property of the estimator $\hat{\tau}_{\text{cml}}(x)$ described in Algorithm 1 in Theorem 3.1.

Theorem 3.1. *When Assumptions 1, 2, 3, and 4 hold, $\sqrt{n}\{\hat{\tau}_{\text{cml}}(x) - \tau(x)\}$ follows an asymptotic normal distribution with mean 0 and variance $\sigma_{x1}^2 = E(f_x)^2$, where*

$$f_x = \frac{I(X = x)}{\pi_x} Y - \frac{I(X = x) - \pi_x}{\pi_x} \mu_x - \tau(x).$$

We remark here that Theorem 3.1 ensures no information loss using sample splitting and cross-fitting, and the asymptotic variance is indeed the same as the variance of the conventional AIPTW estimator as if the true propensity score and conditional mean are known (Robins et al. 1994). On the other hand, in order to successfully incorporate information from the auxiliary data without introducing any bias into the causal model, we require an extra assumption.

Assumption 5 (homogeneous population). There exist parameter values $\boldsymbol{\theta}_*$ such that $E\{\mathbf{H}(\boldsymbol{\theta}_*)\} = \mathbf{0}$.

Assumption 5 requires that the first moment of the “working” estimating function $\mathbf{H}(\boldsymbol{\theta}_*)$ equals zero given some parameter values $\boldsymbol{\theta}_*$. Without the need to correctly model the outcome, the “working” estimating function could be in any form that is mis-specified but follows the zero moment condition. For instance, Assumption 5 requires a unique marginal mean θ_* of outcomes in both the main and auxiliary data when the function $\mathbf{H}(\boldsymbol{\theta})$ takes the form with $h(\theta) = Y - \theta$. This is guaranteed if the main and auxiliary data are from the same population. Thus, this assumption can be viewed as a homogeneous population

assumption. Theorem 3.2 summarizes the asymptotic property of the estimator $\hat{\tau}_{\text{cmlib}}(x)$ described in Algorithm 1.

Theorem 3.2. *When Assumptions 1, 2, 3, 4, and 5 hold, $\hat{\tau}_{\text{cmlib}}(x)$ is a consistent estimator, and $\sqrt{n}\{\hat{\tau}_{\text{cmlib}}(x) - \tau(x)\}$ has an asymptotic normal distribution with mean 0 and variance σ_{x2}^2 satisfying*

$$\sigma_{x2}^2 = \sigma_{x1}^2 - \rho \mathbf{M}_x \mathbf{S} \mathbf{M}_x^\top, \text{ for } x = 0, \dots, L, \quad (9)$$

where $\rho = \lim_{n \rightarrow \infty} 1 - n/N$ is a constant satisfying $0 < \rho < 1$; σ_{x1}^2 is as defined in Theorem 3.1; $\mathbf{M}_x = E(f_x \mathbf{h}^\top)$, and $\mathbf{S} = \{E(\mathbf{h} \mathbf{h}^\top)\}^{-1}$.

This theorem demonstrates the efficiency gain achieved by integrating auxiliary data without introducing bias and maintaining the robustness property in $\hat{\tau}_{\text{cml}}(x)$. We can clearly see that the efficiency gain will gradually increase as the ratio n/N decreases. This means that auxiliary data of a larger size will contribute more to the causal estimation based on the main data. We also observe in numerical studies that auxiliary data of a moderate size already considerably reduces the empirical standard deviation of the estimator $\hat{\tau}_{\text{cmlib}}(x)$ compared with the estimator $\hat{\tau}_{\text{cml}}(x)$ (Table 2). Moreover, we emphasize that to obtain the estimator $\hat{\tau}_{\text{cmlib}}(x)$, the nuisance parameters $\boldsymbol{\theta}$ should be estimated by empirical likelihood (Qin & Lawless 1994), which requires a complicated computational strategy. The following corollary provides an alternative but efficient way to solve the nuisance parameters $\boldsymbol{\theta}$.

Corollary 3.2.1. *(Equivalence in nuisance parameter estimation). Given the same assumptions as in Theorem 3.2, the $\boldsymbol{\theta}$ estimator solved by the constrained optimization in (6) is asymptotically equivalent to the estimator solved by $\sum_{i=1}^N \mathbf{h}_i(\boldsymbol{\theta}) = \mathbf{0}$.*

Thus, instead of applying a conventional empirical likelihood procedure, we can first calculate $\hat{\boldsymbol{\theta}}$ by $\sum_{i=1}^N \mathbf{h}_i(\boldsymbol{\theta}) = \mathbf{0}$ and then plug the estimator back in to obtain the weights

\hat{p}_i by the numerical procedure described in Section 1 of the Supplementary Material; this approach is computationally much faster and more convenient compared to the standard empirical likelihood procedure. We have also evaluated more theoretical properties, such as the optimal use of auxiliary data, and described one extension where only summary statistics are available in the auxiliary data. We refer readers to Section 1.4 and 4 of the Supplementary Material for more details.

The asymptotic variances in Theorems 3.1 and 3.2 require prior knowledge of the true propensity score and the true conditional mean, which are typically unknown when we are considering multiple candidate algorithms. To robustly estimate the standard error, a bootstrapping algorithm is suggested as an alternative approach. To guarantee independent validation, we fix all tuning parameters in estimation based on bootstrapped data. The pseudo-code is summarized in Algorithm S1 in the Supplementary Material.

4 BAG profiled by alcohol intake frequency

Mende (2019) summarized the effect of alcohol consumption on cognitive decline and pointed out that heavy drinkers may result in cognitive decline, but mild-to-moderate drinking may not. In a meta-analysis, Zhao et al. (2023) reported that low or moderate alcohol intake showed no significant association with all-cause mortality risk, whereas an increased risk was observed at higher consumption levels. In our application, we further investigated the impact of alcohol consumption frequency on changes in brain plasticity in the ageing brain (Figure 1B). Instead of using cognition or mortality that are consequences of brain ageing, the primary outcome in our work was the BAG, a direct measure of the difference between brain age and chronological age (Smith et al. 2019, Mo et al. 2022). We were interested in estimating the mean potential outcome of BAG, of which a value larger

than zero may indicate brain ageing in relation to chronological age.

Prediction of BAG and levels of alcohol consumption. The white matter BAG (or brain age) is unobserved in practice but could be predicted by treating white matter imaging data as predictors and chronological age as the outcome (Smith et al. 2019, Mo et al. 2022). Following Smith et al. (2019), this prediction model was built and tuned using a preliminary independent dataset based on a machine learning model and then used to predict brain age for the rest of data. To alleviate the issue of regression towards the mean, we followed the rule of Smith et al. (2019) and calculated adjusted brain age. We refer readers to Section 3 of the Supplementary Material for more details of processing image data and predicting the outcome. To profile BAG among drinkers with different levels of alcohol consumption, we conducted our analysis based on three exclusive subgroups: heavy drinkers (almost daily), moderate drinkers (a few times a week), and light/never drinkers (a few times a month or less). These alcohol consumption frequencies were obtained based on surveys from the UK Biobank study. We did not consider the never drinkers as a separate category due to the small sample size in this category.

Phenomic variables and auxiliary data. We considered phenomic variables as potential confounders that systematically characterized the social, health, and physical conditions of participants, including demographics (age, gender, education, household income, body mass index), nutrition intake (cooked/raw vegetables and/or fruits), blood biochemistry (28 measures), physical activity (7 measures), nuclear-magnetic-resonance metabolomics (167 measures), and urine assays (3 measures). These variables were all measured at the baseline to avoid potential for reverse causality. We additionally used the baseline alcohol intake frequency and a baseline cognition metric (mean time to correctly identify matches from cognition tests) to account for initial brain conditions. As demon-

strated in simulation (Table 2,3), including too many confounders may increase estimation bias. Also due to high missingness in blood biochemistry, metabolomics, and physical measures, including all may further reduce the sample size in the main data. Thus, we introduced a pre-screening step to identify more plausible confounders showing significant Spearman correlation with both outcomes and exposures (Mukaka 2012). After screening, there were 98 confounders remained. Owing to missingness in the remaining confounders (see Section 2.1 of the Supplementary Material), there were in total 2877 participants who had a complete set of data (549 for heavy drinkers, 1661 for moderate drinkers, and 667 for light/never drinkers). We regarded this cohort as our main data. A summary of the studied population was presented in Table S1 of the Supplementary Material. In addition to the main data, there were 18643 participants who missed all or partial phenomic data, treated as auxiliary data. We reported results based on our proposed methods, CML and CMLIB, as well as four competing methods including simple average, AIPTW.Preg, AIPTW.RF, AIPTW.GB, where the same learning and tuning procedures were adopted as demonstrated in Section 5.2. To alleviate potential heterogeneity between the main and auxiliary data, we conducted PS matching with matching ratio 1 : 5, i.e., five auxiliary samples matched to one main sample without replacement, based on demographic variables. As shown in Table S2, there was little difference between the matched cohorts.

Sensitivity analysis. To enhance the robustness and rigor of our findings, we performed four sensitivity analyses. (1) We compared the results without the step of matching the main and the auxiliary data. (2) To evaluate the impact of pre-screening on results, we conducted the analysis using all potential confounders without screening. (3) Given ongoing debates on BAG definition and calculation (Butler et al. 2021), we assessed the robustness of our findings by using another method to calculate BAG (Klemra & Doubal

2006) and re-evaluate impact of alcohol consumption frequency. (4) We used reaction time change from the baseline from cognition assessment as a secondary outcome to validate our findings. We refer readers to Section 2.2 to 2.5 in the Supplementary Material for more details.

Results. The estimated mean potential outcomes (the counterfactual BAG under heavy/moderate/light alcohol intake frequency) were summarized in Table 1. The estimator with information integration had smaller bootstrapped standard deviation compared with the others. On the other hand, all the estimators showed little evidence of mean BAG significantly different from zero in the “light/never” group. This implies that there may be no significant or very little effect of alcohol drinking on ageing of the brain if an individual consumes alcohol in a low frequency per month. However, the estimators including AIPTW.RF, AIPTW.GB, CML, and CMLIB showed at least weak evidence ($P < 0.1$) of mean BAG significantly larger than zero for the “heavy” group. This implies that everyday intake of alcohol has a non-negligible effect on ageing of the brain. It was worth noticing that the CMLIB estimator showed significant effects on ageing the brain for both “heavy” ($P = 0.044$) and “moderate” groups ($P = 0.003$), where the former showed an average increase of 0.7 of a year (8 – 9 months), and the latter showed an average increase of 0.2 of a year (2 – 3 months).

Furthermore, our sensitivity analyses yielded results that highly resemblant to the primary analysis results, reaching to consistent conclusions. Specifically, sensitivity analysis (1) showed almost identical results (Table S3), while (2) showed a similar result pattern with a slightly reduced BAG for “heavy” group compared to the primary analysis (on average increase of 0.34 of a year, Table S4). Sensitivity analysis (3) based on an alternative BAG prediction method indicates that daily alcohol consumption could lead to a significant

acceleration of brain aging by 2.63 years (Table S5). In contrast, groups with lower drinking frequencies might not experience a significant impact on brain age. Lastly, findings based on the cognition metric in (4) revealed that the group of heavy drinkers had the largest mean reaction time change from the baseline, while the other two groups showed similar mean changes (Table S6,S7).

5 Simulation

5.1 Data generation

For illustration in the manuscript, we examined a scenario involving a 2-level exposure (i.e., $X = 0, 1$) with two setups— one with a small number ($p = 10$) and the other with a large number of candidate confounders ($p = 200$), where 5 of them are true confounders. More situations, such as a 3-level exposure (i.e., $X = 0, 1, 2$), more number of true confounders, and the utilization of alternative working functions, are evaluated and discussed in Section 3 of the Supplementary Material. For subject $i = 1, \dots, n$ in the main data, we first generated confounders \mathbf{Z} following a p -variate normal distribution with mean 0, variance 1, and uniform correlation coefficients 0.5 between each pair of confounders. We then generated the potential outcome $Y(x)$ following a normal distribution with conditional mean $\mu_x = E(Y(x) | \mathbf{Z})$ and variance 1, and the exposure X following a Bernoulli distribution with success probability $\pi_x = P(X = x | \mathbf{Z})$. For each dimensional set-up of \mathbf{Z} , we considered the following three cases where the true PS and CM have different mean structures (i.e., linear and complex non-linear).

Case 1 (both linear). $\mu_{xi} = 0.5x + (Z_{i1} + Z_{i2} + Z_{i3} + Z_{i4} + Z_{i5})(0.5x + 1)$ and $\pi_{xi} = \{1 + \exp(-0.5Z_{i1} + 0.5Z_{i2} - 0.5Z_{i3} + 0.5Z_{i4} - 0.5Z_{i5})\}^{-1}$.

Case 2 (non-linear propensity score model). $\mu_{xi} = 0.5x + (Z_{i1} + Z_{i2} + Z_{i3} + Z_{i4} + Z_{i5})(0.5x + 1)$ and $\pi_{xi} = \{1 + \exp(1 - Z_{i1} + 0.5Z_{i2}^2 - \text{abs}(Z_{i3}) + 0.5Z_{i4}Z_{i5})\}^{-1}$, where $\text{abs}(\cdot)$ denotes the absolute value of a given quantity.

Case 3 (both non-linear). $\mu_{xi} = 0.5x + [0.5\{Z_{i1} + 0.5Z_{i2}^2 + Z_{i2}Z_{i3} + Z_{i3} + I(Z_{i4} > 0.3) + Z_{i4} * I(Z_{i5} > 0)\}](0.5x + 1)$ and $\pi_x = \{1 + \exp(1 - Z_{i1} + 0.5Z_{i2}^2 - \text{abs}(Z_{i3}) + 0.5Z_{i4}Z_{i5})\}^{-1}$.

For subject $i = n + 1, \dots, N$ in the auxiliary data, we adopted the same data generating mechanism, except that we made \mathbf{Z}_i a vector of unobserved confounders in the auxiliary data. The above data generation process guarantees a homogeneous population. By contrast, we also considered a set-up with heterogeneity between the main and auxiliary data. We refer readers to Section 3.1 of the Supplementary Material for the detailed data generation procedure. In all three cases, we conducted 500 Monte Carlo runs. For each replicate, we considered sample size $n = 1000, 2000$ for the main data and sample size $2n, 10n$ for the auxiliary data.

5.2 Competing methods and evaluation

We implemented our two proposed estimators: the robust estimator described in Section 3.2 without information integration (CML); and the estimator proposed in Section 3.3, which is expected to be robust and more efficient owing to borrowing information from the auxiliary data (CMLIB). We compared the performance of our proposed estimators with that of the simple average estimator (Raw) and three competing methods that use AIPTW estimator with different algorithms for estimating the nuisance parameters: (1) fit l_2 -penalized logistic regression to the PS model and l_2 -penalized linear regression to the CM model (AIPTW.Preg) with tuning parameters chosen by five-fold cross-validation; (2) use random forest that averages over 1000 trees to learn the PS model and the CM model

(AIPTW.RF); (3) use gradient boosting to learn the PS model and the CM model, with regularization parameters chosen by ten-fold cross-validation (AIPTW.GB). Our CML and CMLIB estimators used all three algorithms including l_2 -penalized regression, random forest, and gradient boosting. We used the form (I) in (7) to facilitate information integration.

We assessed the performance of all estimators based on bias, Monte Carlo variance, bootstrapped standard deviation, and 95% coverage probability. We only present the results for the group of $x = 1$ in the manuscript. Other results, such as those for the group of $x = 0$ as well as mean differences, can be found in Section 3 of the Supplementary Material.

5.3 Results

Table 2 presents the estimation bias where the sample size ratio between the auxiliary data and the main data was 2. Given a small number of confounders ($p = 10$), we found that all existing methods had small estimation bias when either the true propensity score or the true conditional mean had linear mean structure. Specifically, compared with the penalized regression-based estimator, the estimator based on gradient boosting had relatively large bias when both the true PS and CM had linear mean structures. This justifies our previous statement that a more complicated algorithm does not necessarily lead to a better estimate given a finite sample size. However, when the mean structures became more complicated, the estimator with gradient boosting became more favourable in terms of having smaller bias. In addition, the estimators based on penalized regression became considerably biased when both PS and CM had non-linear mean structures. When the number of confounders increased ($p = 200$), the bias became larger for all estimators, yet similar patterns were observed among competing methods. In contrast, our proposed estimators (CML and

CMLIB) consistently exhibited little bias and had the most stable performance, irrespective of the dimensionality of confounders and the complexity in the true PS and CM.

Table 2 also summarizes the estimation variability. We found that the variability of the CML estimator was comparable with that of other machine-learning-based estimators, whereas the CMLIB estimator had considerably smaller variability compared with the others. When the sample size of the auxiliary data increased from $2n$ to $10n$, the efficiency gain became higher (Table 3). Moreover, the bootstrapped standard deviation was close to the empirical standard deviation, which validates the proposed bootstrapping strategy (Table 4). The 95% coverage probability became closer to its nominal level in most cases as the sample size increased to 2000. Owing to some bias, the coverage probability was under 95% in the case where both the true PS and CM had complex non-linear structures with numerous confounders.

All the results above rely on a set-up where the main data and auxiliary data are from the same population. We also evaluated the impact of heterogeneous populations on information integration with and without a matching step before estimation. Specifically, we used observed confounders in both data and applied PS matching between the main data and the auxiliary data based on the nearest-neighbour rule and a matching ratio of $1 : 2$, i.e., two auxiliary samples matched one main sample without replacement. Table S8 in Section 2 of the Supplementary Material summarizes the results. As shown in the table, heterogeneous populations caused substantial bias for the CMLIB estimator before PS matching. However, after implementing PS matching, there was little bias but substantial efficiency gain. These findings validate the use of matching in real applications where two studied populations are potentially different. In addition, we also observe consistent patterns in results for the control group (Table S9 and S11) as well as two-group differences

(Table S10 and S12).

Furthermore, we assessed additional scenarios, including a 3-level exposure (Table S15-S17), a greater number of true confounders (Table S13), and the exploration of alternative working functions (Table S14), to mimic different setups in real applications. All these scenarios exhibited patterns and results similar to those presented in the manuscript. For more details, please refer to Section 3 of the Supplementary Material.

6 Discussion

This work proposes a useful toolbox that implicitly and effectively achieves model ensemble and produces a consistent, robust, and efficient mean potential outcome estimation. This method can also be used to conduct group comparisons. The usability of the toolbox is further improved by integrating information from the auxiliary data, where massive phenomic variables are completely missing or only partially observed. This type of auxiliary data is commonly seen or easily constructed in real studies.

By applying this tool, we have successfully depicted the profiles of alcohol consumption influencing the ageing brain. We find that individuals who consumed alcohol daily exhibited the largest adverse effect on brain ageing. Furthermore, our findings suggest that moderate alcohol intake (i.e., a few times a week) may also contribute to accelerated brain ageing. The brain ageing trend of light/never drinkers is close to the normalcy. Our findings are well aligned with the conclusion from a recent study in Zhao et al. (2023) that even moderate levels of alcohol intake might be detrimental in terms of all-cause mortality. Our study furthermore offers insights from the perspective of brain aging and drinking frequency with quantitative evaluations. These jointly consolidate valuable evidence to the understanding of the causal relationship between alcohol consumption and brain health, which provides

potential guidance for the prevention of accelerated neurodegeneration during ageing.

Although this article considers the case where the raw auxiliary data are available, the proposed method can be extended to the situation where only summary information of auxiliary data is available. Also, our method could be extended to more sophisticated causal models, such as marginal structure models handling binary outcome and time-varying exposures, all of which merit future work. When the main data and auxiliary data are random samples from different populations, we advocate the use of matching before implementing the proposed learner. Another solution to alleviate data heterogeneity is to specify different working functions \mathbf{h}_1 and \mathbf{h}_2 in (6). We refer readers to Section 4 of the Supplementary Material for details.

References

- Antonelli, J., Cefalu, M., Palmer, N. & Agniel, D. (2018), ‘Doubly robust matching estimators for high dimensional confounding adjustment’, *Biometrics* **74**(4), 1171–1179.
- Bang, H. & Robins, J. M. (2005), ‘Doubly robust estimation in missing data and causal inference models’, *Biometrics* **61**(4), 962–973.
- Butler, E. R., Chen, A., Ramadan, R., Le, T. T., Ruparel, K., Moore, T. M., Satterthwaite, T. D., Zhang, F., Shou, H., Gur, R. C. et al. (2021), Pitfalls in brain age analyses, Technical report, Wiley Online Library.
- Chatterjee, N., Chen, Y.-H., Maas, P. & Carroll, R. J. (2016), ‘Constrained maximum likelihood estimation for model calibration using summary-level information from external big data sources’, *Journal of the American Statistical Association* **111**(513), 107–117.

- Chen, C., Han, P. & He, F. (2022), ‘Improving main analysis by borrowing information from auxiliary data’, *Statistics in Medicine* **41**(3), 567–579.
- Chen, C., Wang, M. & Chen, S. (2023), ‘An efficient data integration scheme for synthesizing information from multiple secondary datasets for the parameter inference of the main analysis’, *Biometrics* .
- Cheng, W., Taylor, J. M., Gu, T., Tomlins, S. A. & Mukherjee, B. (2019), ‘Informing a risk prediction model for binary outcomes with external coefficient information’, *Journal of the Royal Statistical Society: Series C (Applied Statistics)* **68**(1), 121–139.
- Chernozhukov, V., Chetverikov, D., Demirer, M., Duflo, E., Hansen, C., Newey, W. & Robins, J. (2018), ‘Double/debiased machine learning for treatment and structural parameters’.
- Cui, Y., Kosorok, M. R., Sverdrup, E., Wager, S. & Zhu, R. (2023), ‘Estimating heterogeneous treatment effects with right-censored data via causal survival forests’, *Journal of the Royal Statistical Society Series B: Statistical Methodology* **85**(2), 179–211.
- Ganaie, M. A., Hu, M. et al. (2021), ‘Ensemble deep learning: A review’, *arXiv preprint arXiv:2104.02395* .
- Han, P. & Wang, L. (2013), ‘Estimation with missing data: beyond double robustness’, *Biometrika* **100**(2), 417–430.
- Hernán, M. A. & Robins, J. M. (2010), ‘Causal inference’.
- Horvitz, D. G. & Thompson, D. J. (1952), ‘A generalization of sampling without replacement from a finite universe’, *Journal of the American statistical Association* **47**(260), 663–685.

- Houle, D., Govindaraju, D. R. & Omholt, S. (2010), ‘Phenomics: the next challenge’, *Nature reviews genetics* **11**(12), 855–866.
- Jiang, L., Nie, L. & Yuan, Y. (2021), ‘Elastic priors to dynamically borrow information from historical data in clinical trials’, *Biometrics* .
- Jiang, Z., Yang, B., Qin, J. & Zhou, Y. (2021), ‘Enhanced empirical likelihood estimation of incubation period of covid-19 by integrating published information’, *Statistics in medicine* **40**(19), 4252–4268.
- Jiang, Z., Yang, S. & Ding, P. (2022), ‘Multiply robust estimation of causal effects under principal ignorability’, *Journal of the Royal Statistical Society Series B: Statistical Methodology* **84**(4), 1423–1445.
- Kang, J. D. & Schafer, J. L. (2007), ‘Demystifying double robustness: A comparison of alternative strategies for estimating a population mean from incomplete data’, *Statistical science* **22**(4), 523–539.
- Klemera, P. & Doubal, S. (2006), ‘A new approach to the concept and computation of biological age’, *Mechanisms of ageing and development* **127**(3), 240–248.
- Kundu, P., Tang, R. & Chatterjee, N. (2019), ‘Generalized meta-analysis for multiple regression models across studies with disparate covariate information’, *Biometrika* **106**(3), 567–585.
- Mende, M. A. (2019), ‘Alcohol in the aging brain—the interplay between alcohol consumption, cognitive decline and the cardiovascular system’, *Frontiers in Neuroscience* **13**, 713.
- Mo, C., Wang, J., Ye, Z., Ke, H., Liu, S., Hatch, K., Gao, S., Magidson, J., Chen, C., Mitchell, B. D. et al. (2022), ‘Evaluating the causal effect of tobacco smoking on white

- matter brain aging: a two-sample mendelian randomization analysis in uk biobank’, *Addiction* .
- Mukaka, M. M. (2012), ‘A guide to appropriate use of correlation coefficient in medical research’, *Malawi medical journal* **24**(3), 69–71.
- Nelder, J. A. & Wedderburn, R. W. (1972), ‘Generalized linear models’, *Journal of the Royal Statistical Society: Series A (General)* **135**(3), 370–384.
- Polley, E. C. & Van der Laan, M. J. (2010), ‘Super learner in prediction’.
- Qin, J. & Lawless, J. (1994), ‘Empirical likelihood and general estimating equations’, *the Annals of Statistics* **22**(1), 300–325.
- Qin, J., Zhang, H., Li, P., Albanes, D. & Yu, K. (2015), ‘Using covariate-specific disease prevalence information to increase the power of case-control studies’, *Biometrika* **102**(1), 169–180.
- Robins, J. M. (1999), ‘Testing and estimation of direct effects by reparameterizing directed acyclic graphs with structural nested models’, *Computation, causation, and discovery* pp. 349–405.
- Robins, J. M., Rotnitzky, A. & Zhao, L. P. (1994), ‘Estimation of regression coefficients when some regressors are not always observed’, *Journal of the American statistical Association* **89**(427), 846–866.
- Rosenbaum, P. R. & Rubin, D. B. (1983), ‘The central role of the propensity score in observational studies for causal effects’, *Biometrika* **70**(1), 41–55.
- Rubin, D. B. (1973), ‘Matching to remove bias in observational studies’, *Biometrics* pp. 159–183.

- Rubin, D. B. (2006), *Matched sampling for causal effects*, Cambridge University Press.
- Sheng, Y., Sun, Y., Huang, C.-Y. & Kim, M.-O. (2022), ‘Synthesizing external aggregated information in the presence of population heterogeneity: A penalized empirical likelihood approach’, *Biometrics* **78**(2), 679–690.
- Smith, S. M., Vidaurre, D., Alfaro-Almagro, F., Nichols, T. E. & Miller, K. L. (2019), ‘Estimation of brain age delta from brain imaging’, *Neuroimage* **200**, 528–539.
- Yang, S. & Ding, P. (2019), ‘Combining multiple observational data sources to estimate causal effects’, *Journal of the American Statistical Association* .
- Yang, S., Gao, C., Zeng, D. & Wang, X. (2023), ‘Elastic integrative analysis of randomised trial and real-world data for treatment heterogeneity estimation’, *Journal of the Royal Statistical Society Series B: Statistical Methodology* **85**(3), 575–596.
- Zhai, Y. & Han, P. (2022), ‘Data integration with oracle use of external information from heterogeneous populations’, *Journal of Computational and Graphical Statistics* pp. 1–12.
- Zhang, H., Deng, L., Schiffman, M., Qin, J. & Yu, K. (2020), ‘Generalized integration model for improved statistical inference by leveraging external summary data’, *Biometrika* **107**(3), 689–703.
- Zhao, J., Stockwell, T., Naimi, T., Churchill, S., Clay, J. & Sherk, A. (2023), ‘Association between daily alcohol intake and risk of all-cause mortality: a systematic review and meta-analyses’, *JAMA Network Open* **6**(3), e236185–e236185.

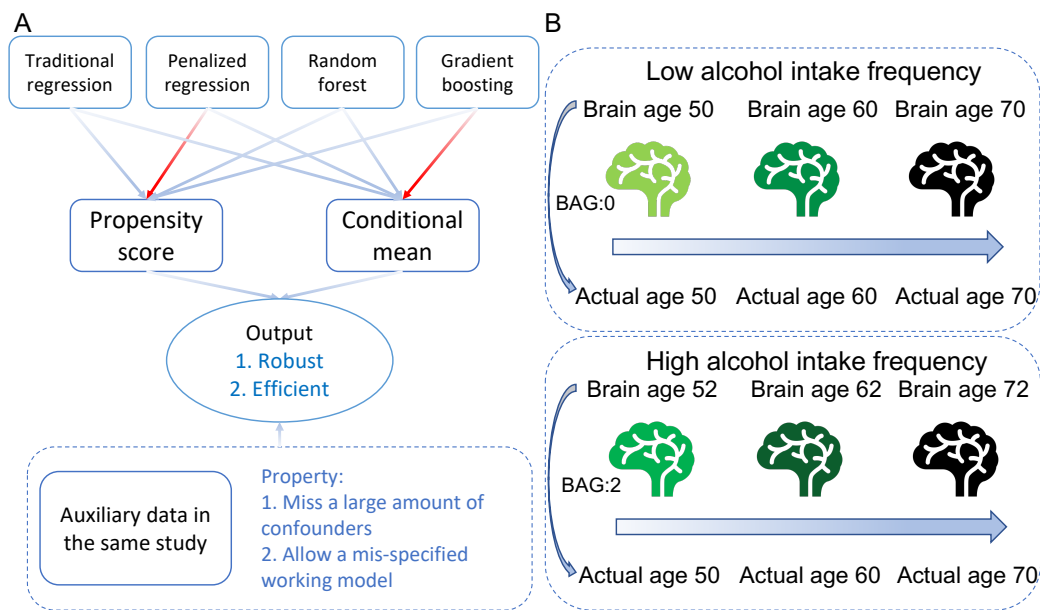


Figure 1: A: a statistical framework of robust machine learner and information integration;

B: a pseudo example of BAG in two cohorts with low and high alcohol intake frequencies.

Table 1: Mean potential outcome estimates of BAG under three alcohol intake frequencies.

		BAG	BSD	95%LL	95%UL	P-value
Heavy	Raw	0.312	0.131	0.055	0.570	0.017
	AIPTW.Preg	0.519	0.666	-0.786	1.824	0.436
	AIPTW.RF	0.344	0.145	0.060	0.627	0.018
	AIPTW.GB	0.638	0.333	-0.014	1.290	0.055
	CML	0.668	0.379	-0.074	1.409	0.078
	CMLIB	0.699	0.348	0.018	1.381	0.044
Moderate	Raw	0.025	0.079	-0.129	0.180	0.749
	AIPTW.Preg	0.085	0.382	-0.663	0.833	0.824
	AIPTW.RF	0.054	0.082	-0.106	0.215	0.508
	AIPTW.GB	0.139	0.183	-0.219	0.498	0.447
	CML	0.125	0.091	-0.054	0.303	0.170
	CMLIB	0.203	0.068	0.070	0.336	0.003
Light/never	Raw	-0.018	0.147	-0.306	0.269	0.900
	AIPTW.Preg	-0.373	0.418	-1.191	0.446	0.372
	AIPTW.RF	0.069	0.146	-0.217	0.356	0.635
	AIPTW.GB	0.083	0.269	-0.445	0.611	0.758
	CML	-0.081	0.268	-0.606	0.444	0.762
	CMLIB	0.019	0.227	-0.426	0.464	0.932

Heavy: daily alcohol intake; Moderate: a few times a week; Light/never: a few times a month or less; BSD: Bootstrapped standard deviation; 95%LL: lower limit of 95% confidence interval; 95%UL: upper limit of 95% confidence interval; Raw: simple average; AIPTW: AIPTW-based estimates with random forest (RF), l_2 penalized regression (Preg), or gradient boosting (GB); CML: the proposed estimator without information borrowing; CMLIB: the proposed estimator with information borrowing.

Table 2: Evaluations of six mean potential outcome estimates ($x=1$) based on 500 Monte Carlo runs, with the main and auxiliary data population sharing the same distribution. The main data sample size is n , and the auxiliary data sample size is $2n$.

		Small				Large			
		n=1000		n=2000		n=1000		n=2000	
		Bias	MCSD	Bias	MCSD	Bias	MCSD	Bias	MCSD
Case 1	Raw	0.979	0.268	0.972	0.192	0.962	0.258	0.961	0.188
	AIPTW.Preg	-0.001	0.198	0.006	0.141	0.120	0.197	0.015	0.141
	AIPTW.RF	0.027	0.204	0.027	0.145	0.139	0.197	0.124	0.140
	AIPTW.GB	0.090	0.201	0.059	0.145	0.154	0.195	0.107	0.144
	CML	-0.002	0.198	0.007	0.141	0.061	0.190	0.011	0.142
	CMLIB	0.004	0.117	0.005	0.087	0.059	0.127	0.010	0.092
Case 2	Raw	1.539	0.282	1.544	0.203	1.526	0.270	1.546	0.194
	AIPTW.Preg	0.000	0.196	0.001	0.142	0.177	0.202	0.020	0.141
	AIPTW.RF	0.056	0.200	0.057	0.144	0.191	0.197	0.184	0.144
	AIPTW.GB	0.086	0.207	0.053	0.148	0.151	0.199	0.105	0.143
	CML	0.000	0.197	0.003	0.143	0.089	0.193	0.018	0.139
	CMLIB	0.010	0.119	0.001	0.088	0.091	0.129	0.014	0.089
Case 3	Raw	0.736	0.127	0.740	0.093	0.743	0.124	0.749	0.091
	AIPTW.Preg	0.362	0.151	0.364	0.106	0.444	0.136	0.397	0.097
	AIPTW.RF	0.048	0.093	0.037	0.070	0.223	0.095	0.193	0.067
	AIPTW.GB	0.036	0.095	0.023	0.073	0.101	0.100	0.056	0.068
	CML	0.019	0.093	0.014	0.071	0.099	0.095	0.065	0.065
	CMLIB	0.024	0.069	0.014	0.051	0.098	0.070	0.063	0.049

Small: 10 confounders; Large: 200 confounders; Case 1: linear mean structures in both the propensity score (PS) and conditional mean (CM); Case 2: non-linear mean structure in PS and linear mean structure in CM; Case 3: non-linear mean structures in both PS and CM; Raw: simple average based on observed data; AIPTW: AIPTW-based estimates with random forest (RF), l_2 penalized regression (Preg), or gradient boosting (GB); CML: the proposed estimator without information borrowing; CMLIB: the proposed estimator with information borrowing; MCSD: Monte Carlo standard deviation.

Table 3: Evaluations of six mean potential outcome estimates ($x=1$) based on 500 Monte Carlo runs, with the main and auxiliary data population sharing the same distribution. The main data sample size is n , and the auxiliary data sample size is $10n$.

		Small				Large			
		n=1000		n=2000		n=1000		n=2000	
		Bias	MCSD	Bias	MCSD	Bias	MCSD	Bias	MCSD
Case 1	Raw	0.966	0.277	0.977	0.174	0.970	0.263	0.957	0.184
	AIPW.Preg	0.004	0.201	-0.002	0.134	0.121	0.193	0.004	0.135
	AIPW.RF	0.030	0.215	0.020	0.137	0.139	0.192	0.116	0.140
	AIPW.GB	0.091	0.211	0.052	0.137	0.150	0.190	0.101	0.139
	CML	0.003	0.202	-0.002	0.134	0.062	0.190	0.001	0.135
	CMLIB	0.003	0.081	-0.002	0.054	0.066	0.087	0.011	0.057
Case 2	Raw	1.546	0.285	1.534	0.188	1.530	0.270	1.534	0.185
	AIPW.Preg	-0.004	0.199	-0.005	0.133	0.169	0.203	0.011	0.135
	AIPW.RF	0.054	0.206	0.051	0.138	0.188	0.198	0.172	0.137
	AIPW.GB	0.088	0.208	0.053	0.142	0.149	0.205	0.086	0.136
	CML	-0.004	0.199	-0.003	0.135	0.087	0.190	0.009	0.133
	CMLIB	-0.004	0.078	-0.001	0.056	0.095	0.086	0.018	0.056
Case 3	Raw	0.740	0.127	0.738	0.086	0.744	0.126	0.737	0.087
	AIPW.Preg	0.369	0.160	0.361	0.100	0.447	0.136	0.390	0.098
	AIPW.RF	0.049	0.096	0.031	0.064	0.223	0.095	0.187	0.067
	AIPW.GB	0.036	0.099	0.016	0.065	0.102	0.101	0.049	0.069
	CML	0.023	0.093	0.007	0.065	0.102	0.096	0.060	0.067
	CMLIB	0.024	0.058	0.008	0.041	0.101	0.060	0.062	0.039

Small: 10 confounders; Large: 200 confounders; Case 1: linear mean structures in both the propensity score (PS) and conditional mean (CM); Case 2: non-linear mean structure in PS and linear mean structure in CM; Case 3: non-linear mean structures in both PS and CM; Raw: simple average based on observed data; AIPW: AIPW-based estimates with random forest (RF), l_2 penalized regression (Preg), or gradient boosting (GB); CML: the proposed estimator without information borrowing; CMLIB: the proposed estimator with information borrowing; MCSD: Monte Carlo standard deviation.

Table 4: Evaluations of bootstrapped standard deviation ($x=1$) based on 100 bootstrapped samples and 500 Monte Carlo runs. The main and auxiliary data populations are the same. The main data sample size is n , and the auxiliary data sample size is $2n$.

			n=1000			n=2000		
			MCS	BSD	CP	MCS	BSD	CP
Small	Case 1	CML	0.195	0.191	93	0.144	0.135	94
		CMLIB	0.118	0.119	96	0.088	0.085	94
	Case 2	CML	0.199	0.192	93	0.142	0.135	94
		CMLIB	0.117	0.119	96	0.086	0.084	93
	Case 3	CML	0.097	0.094	93	0.068	0.066	95
		CMLIB	0.072	0.071	93	0.049	0.049	95
Large	Case 1	CML	0.192	0.197	93	0.141	0.137	95
		CMLIB	0.127	0.130	93	0.091	0.087	93
	Case 2	CML	0.190	0.199	93	0.140	0.137	93
		CMLIB	0.131	0.133	89	0.090	0.087	93
	Case 3	CML	0.092	0.097	84	0.068	0.068	85
		CMLIB	0.071	0.074	75	0.050	0.051	79

Small: 10 confounders; Large: 200 confounders; Case 1: linear mean structures in both PS and CM; Case 2: non-linear mean structure in PS and linear mean structure in CM; Case 3: non-linear mean structures in both PS and CM; CML: the proposed estimator without information borrowing; CMLIB: the proposed estimator with information borrowing. MCS: Monte Carlo standard deviation; BSD: bootstrapped standard deviation; CP: coverage probability based on 95% confidence interval.